

BENCHMARKING OF THE JEF2.2 DATA LIBRARY FOR SHIELDING APPLICATIONS

G.A.Wright	A.F.Avery	M.J.Grimstone	H.F.Locke	S.Newbon
AEA Technology	AEA Technology	AEA Technology	AEA Technology	AEA Technology
Dorchester	Dorchester	Dorchester	Dorchester	Dorchester
Dorset	Dorset	Dorset	Dorset	Dorset
United Kingdom	United Kingdom	United Kingdom	United Kingdom	United Kingdom

ABSTRACT

The recently released JEF2.2 nuclear data library is currently being benchmarked for shielding applications in the UK by analysing shielding benchmark experiments using the Monte Carlo radiation transport code MCBEND. Four analyses are described, three for single material benchmarks in iron, graphite and water and one for an iron/water benchmark simulating the radial shield of a PWR. Comparisons with experiment and with results using UKNDL data are made. The JEF2.2 data for iron, hydrogen, oxygen and carbon all appear to be good at energies in the 3MeV-9MeV region but the comparisons suggest that there may be inaccuracies in the data for iron between 0.6MeV and 1.4MeV and for carbon between 0.8MeV and 2.9MeV. The JEF2.2 iron data is an improvement over UKNDL data whilst for carbon the data gives improved agreement at high energies but worse at intermediate energies. Investigation of resonance shielding effects shows that a 1/128 lethargy width energy group scheme is not fine enough to be equivalent to point energy in the Fe56 resonance region, the effect on reaction rates being significant in the iron benchmark.

I. INTRODUCTION

The JEF2.2 nuclear data library was released in 1992 and is currently being benchmark tested by the participants in the JEF project. The UK contribution to benchmarking the data for shielding applications is to use the Monte Carlo code MCBEND to analyse single material and multi-material benchmark experiments performed at AEA Technology, Winfrith.¹ These experiments have very well defined sources, geometries and material compositions so that they can be modelled with very little uncertainty using the Monte Carlo method. The experiments analysed to date include single material iron, graphite and water benchmarks and an iron/water benchmark simulating a PWR radial shield (NESDIP2). The Monte Carlo method is chosen to validate the data since errors in modelling the experiment and in representation of the nuclear data are minimised. Results, together with sensitivity profiles calculated

concurrently with reaction rates, are made available to the JEF Working Group for inclusion in an overall database to be used to make recommendations concerning improvements to the data. Results are also compared, where possible, with previous analyses using UKNDL data to assess the effects of changing the data library.

II. DESCRIPTION OF THE EXPERIMENTS

Three of the four experiments analysed (iron, graphite and NESDIP2 benchmarks) were performed in the ASPIS facility of the NESTOR reactor whilst the fourth, the water benchmark, was performed in a large water tank using a ring of Cf252 sources.

A. ASPIS Shielding Facility

The ASPIS shielding facility is installed on the NESTOR reactor at Winfrith. NESTOR is a light water cooled, graphite and light water moderated reactor which operates at powers of up to 30kW and is used as a source of neutrons for a wide range of applications. The core of the reactor, which comprises 26 MTR (Materials Test Reactor) type fuel elements, is contained within an annulus formed by two concentric aluminium vessels through which water circulates. The inner vessel is filled with graphite to form an inner reflector. The outer tank is surrounded by an external graphite reflector in the form of a block having dimensions 182cm x 182cm x 122cm which contains the control plate slots adjacent to the vessel wall. Leading off each of the four faces of the external reflector is an experiment cave which can be isolated from the reactor by shutters composed of boral or combinations of neutron/gamma-ray shield materials.

ASPIS is located in the NESTOR cave C. Shield components, which are in the main slabs or tanks, are mounted vertically in a mobile tank which has an internal cross-sectional area of 1.8m x 1.9m and a length of 3.7m. A fission plate manufactured from 93% enriched uranium/aluminium alloy is located within the experimental shield array. The loaded tank is moved into

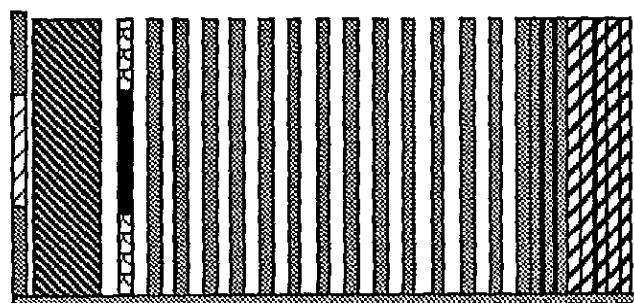
Wright

14080183

the cave where thermal neutrons leaking from the outer graphite reflector of NESTOR are used to drive the fission plate to provide a well defined neutron source for penetration measurements. The absolute source strength is determined to a precision of 4% by fission product counting and the spatial distribution is determined via detailed low energy flux mapping with activation detectors. For the iron and iron/water benchmarks the fission plate approximates to a disc source with an effective radius of 56cm and a thickness of 2mm whilst for the graphite benchmark the fission plate gives a rectangular source of approximately 40cm x 60cm with effective thickness 4mm. A fraction of the neutrons present in the ASPIS experimental array originate from leakage from the NESTOR core. To obtain a true comparison between measurement and a calculation using the fission plate source, the NESTOR core component must be subtracted from the measurement.

B. Iron Benchmark

The iron benchmark experimental array is shown schematically in side elevation in Figure 1. The array comprises three regions; the source region containing moderator and the fission plate, the shield made from 13 mild steel plates, each of approximately 5.1cm thickness, and a deep backing shield manufactured from mild and stainless steel. Each plate is 1.8m x 1.9m in cross-section, thus filling the mobile tank described above. To allow detector access within the shield 6mm spacers are placed between each plate. Measurements of the reaction rates $S32(n,p)P32$, $In115(n,n')In115m$, $Rh103(n,n')Rh103m$ and $Au197(n,\gamma)Au198/Cd$ were made in activation foils along the nuclear centre line, providing information on high, intermediate and low energy ranges of the spectrum.



All components are 182.9cm wide by 191.0cm high Not To Scale

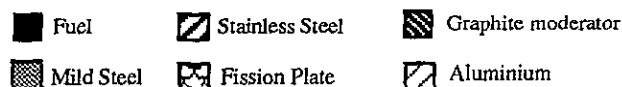


Figure 1 Iron Benchmark Experiment

C. Graphite Benchmark

The configuration of the graphite benchmark experiment is shown schematically in Figure 2. The shield consists of graphite blocks of varying dimensions which are placed in the mobile tank to give a total thickness of 177cm. There is a central cylindrical plug of radius 6.5cm which is fitted into a hole machined out of a rectangular central block 15.6cm x 17.8cm. Slots are cut into this plug at 10cm intervals to provide access for detector foils. The plug is inserted into the central block with foils in place, the shield is irradiated and the plug withdrawn and foil activities counted. Measurements of the reaction rates $S32(n,p)P32$, $In115(n,n')In115m$ and $Rh103(n,n')Rh103m$ were made in activation foils at shield penetrations of up to 70cm, providing information on both high and intermediate energy ranges of the spectrum.

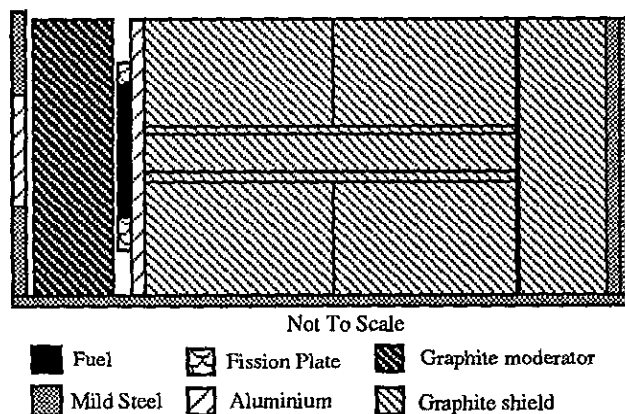


Figure 2 Graphite Benchmark Experiment

D. Water Benchmark

The configuration for the water benchmark is shown in Figure 3. The experiment consisted of a water tank into which was placed an aluminium frame from which were

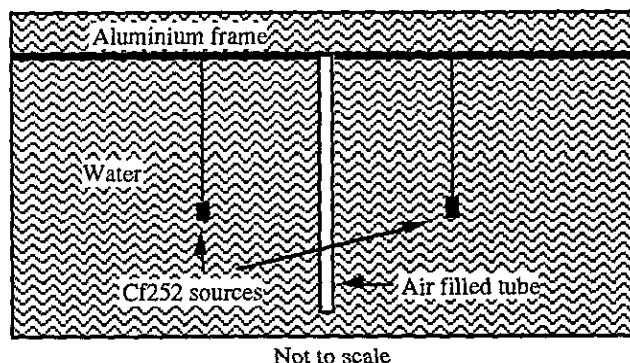
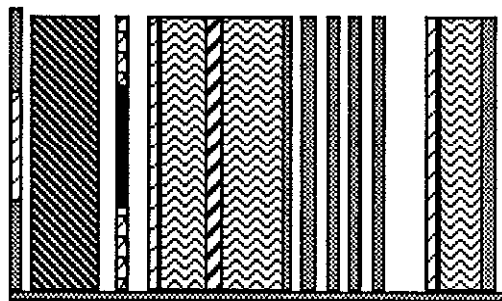


Figure 3 Water Benchmark Experiment

hung a number of Cf252 sources, all equal distances from a measuring tube on the central axis in which $S32(n,p)P32$ reaction rates and neutron spectra above 1MeV were measured. The distance of the sources from the central axis could be varied from 10.2cm to 50.8cm in 5.1cm steps. The absolute strengths of the sources were measured to a precision of 0.5% at the National Physical Laboratory using the manganese bath method.

E. NESDIP2 Benchmark

The NESDIP2 benchmark experimental array is shown schematically in Figure 4. The shield simulates the radial shield of a PWR and consists of 12.1cm of a water, a 5.9cm stainless steel plate simulating the thermal shield, 13.2cm of water, five mild steel plates giving a thickness of 22.8cm to simulate the pressure vessel, a 29.6cm cavity region and a backing shield of aluminium, water and mild steel. Measurements of the reaction rates $S32(n,p)P32$, $In115(n,n')In115m$ and $Rh103(n,n')Rh103m$ were made in activation foils between the mild steel plates and in the cavity whilst $Rh103(n,n')Rh103m$ measurements were also made through the water regions.



All components are 182.9cm wide by 191.0cm high Not To Scale

Fuel Stainless Steel Graphite Water
 Mild Steel Fission Plate Aluminium

Figure 4 NESDIP2 Benchmark Experiment

III. DESCRIPTION OF THE CALCULATIONS

The four benchmarks have been analysed using the general purpose Monte Carlo radiation shielding code MCBEND. This code is well suited to the task of benchmarking nuclear data since bias due to geometry and energy modelling is minimised. In addition to predicting detector foil count rates and spectra MCBEND has also been used to predict the sensitivity of detector count rates to the basic nuclear data. The sensitivities are generated during the main calculation using the DUCKPOND module with a small time penalty: no extra calculations or

adjoint calculations are required.² The following sections describe various aspects of the calculations.

A. Nuclear Data

The nuclear data for the MCBEND calculations are held in 8220 energy groups. This group scheme is used both for criticality and shielding calculations and is particularly fine below 72eV in order to represent the resonance structure in heavy elements. In the energy region from 72eV upwards the groups each have a lethargy width of 1/128. The JEF2.2 data was processed into the 8220 group scheme using a version, NJOY89.62W, of the NJOY89 code.³

For all shielding nuclides except Fe56 the 8220 group scheme is expected to be fine enough to be equivalent to point energy and so the weighting spectrum used to collapse the basic data to this group scheme should not affect the results (i.e. no within-group resonance shielding effects should be present). For these nuclides a 1/E spectrum was used above 1eV.

For Fe56, however, with the problematic unresolved resonance region above 0.85MeV, some account needs to be taken of resonance shielding, even with this fine energy group scheme. Totally shielded cross-sections using $1/(E\Sigma_t)$ weighting are appropriate to slowing down in a material whereas shield calculations involve penetration through a region. The correct weighting spectrum is thus spatially dependent and neither 1/E nor $1/(E\Sigma_t)$ are correct even for materials with single isotopes. However, when the energy group scheme is not equivalent to point energy then the use of the totally shielded cross-section is the best available approximation and $1/(E\Sigma_t)$ weighting was used above 1eV in this work. In addition the Fe56 data was also processed using the 1/E spectrum so that the magnitude of the within-group resonance shielding effect in Fe56 for the 8220 energy group scheme could be assessed by comparing results obtained with the two different weighting spectra.

B. Geometry, Source and Material Modelling

The dimensions and material compositions of the shield components of each experiment were accurately measured and modelled exactly in MCBEND. The measured absolute source strengths of the fission plates and of the Cf252 sources were included in the models and the source profiles for the fission plates derived from foil measurements over the face of the plate were represented accurately. JEF2.2 data is held for individual isotopes rather than for natural elements so for iron, chromium and nickel the natural element had to be divided into isotopic content.

C. Detector Cross-Sections

The detector cross-sections, or response functions, used to evaluate the $S32(n,p)P32$, $In115(n,n')In115m$, and $Rh103(n,n')Rh103m$ reaction rates were taken from the MCBEND response function library which contains these responses in 641 groups and is sourced from the IRDF dosimetry file.⁴ The response function for the $Au197(n,\gamma)Au198/Cd$ reaction rate was in suppressed form, specific to the thickness of the detector foils which were used.

D. Variance Reduction

The standard MCBEND technique of splitting and Russian Roulette was used to accelerate the calculations; for the water benchmark source weighting was also used. The automatic acceleration option of MCBEND (MAGIC) was used to provide the importances for splitting/Russian roulette.⁵ The calculations were generally run to achieve 3% or better standard deviations on the detector count rates.

IV. RESULTS

Figures 5-19 show the results for the four benchmarks. In all of these figures the error bars are at the one standard deviation level and generally include Monte Carlo and detector counting statistics only, exceptions being mentioned in the text.

A. Iron Benchmark

Figures 5-8 show ratios of calculated to measured reaction rates (C/M values) obtained for the four detectors used in the iron benchmark for both JEF2.2 and UKNDL data. The JEF2.2 data clearly give improved results compared with UKNDL data and the agreement with experiment for the $S32(n,p)P32$, $Rh103(n,n')Rh103m$ and $Au197(n,\gamma)Au198/Cd$ detectors is good. However, there is still a marked overprediction of the attenuation of the $In115(n,n')In115m$ reaction rate through the shield. The discrepancy remains even when all other sources of uncertainty (nuclear data, source strength, detector cross-section and fission spectrum) are taken into account. Figure 9 shows the sensitivity of the $S32(n,p)P32$, $In115(n,n')In115m$ and $Rh103(n,n')Rh103m$ reaction rates after 46cm penetration to the total iron cross-section. These sensitivities, combined with the detector results indicate qualitatively that there may be a possible problem with the JEF2.2 iron cross-sections in the energy range 0.6MeV to 1.4MeV, in which the indium sensitivities are high relative to those for sulphur and rhodium.

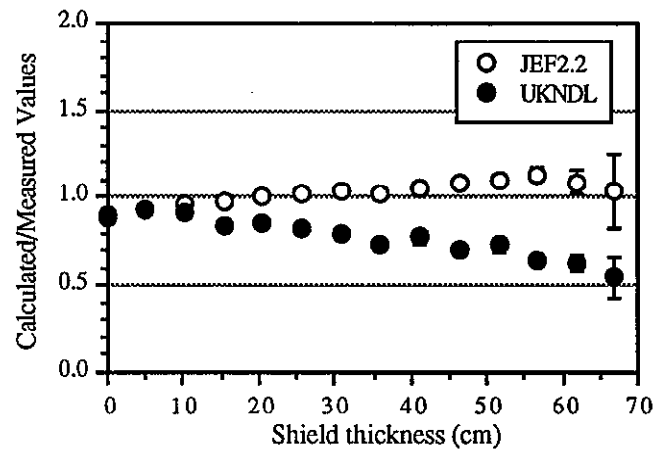


Figure 5 Iron Benchmark C/M Values for S32 Detector

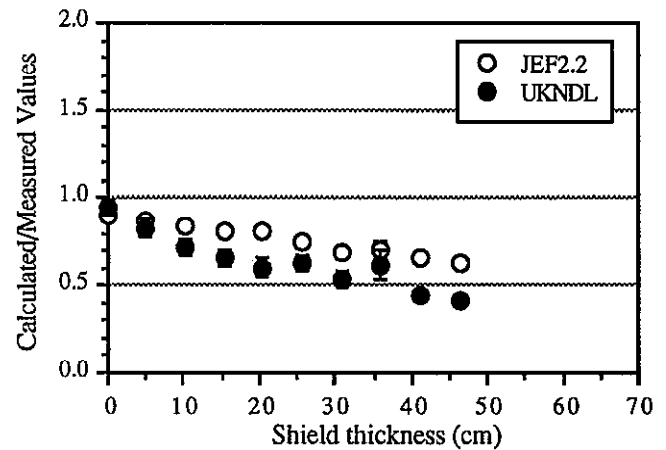


Figure 6 Iron Benchmark C/M Values for In115 Detector

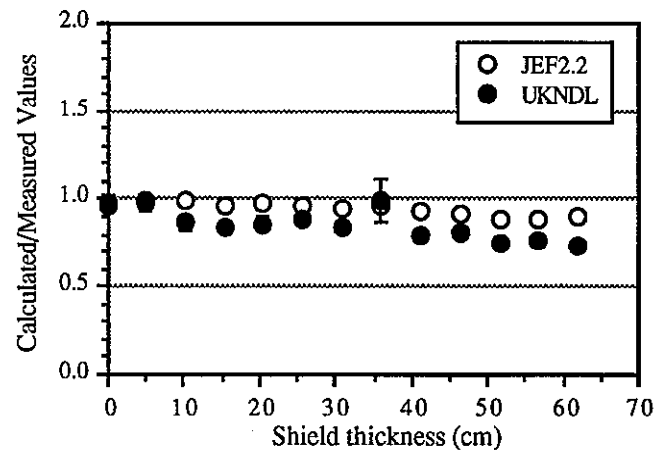


Figure 7 Iron Benchmark C/M Values for Rh103 Detector

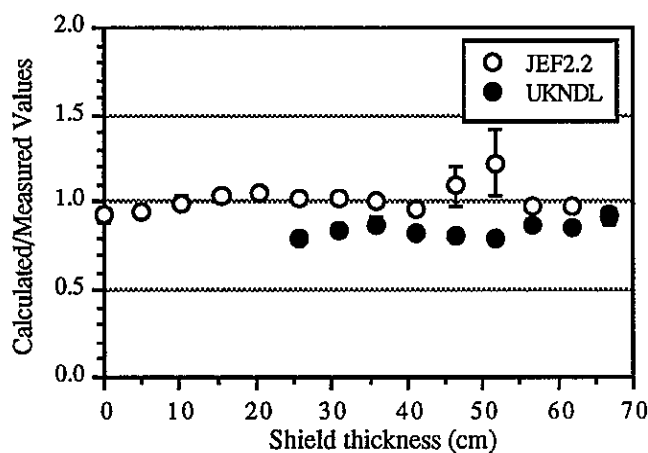


Figure 8 Iron Benchmark C/M Values for Au197 Detector

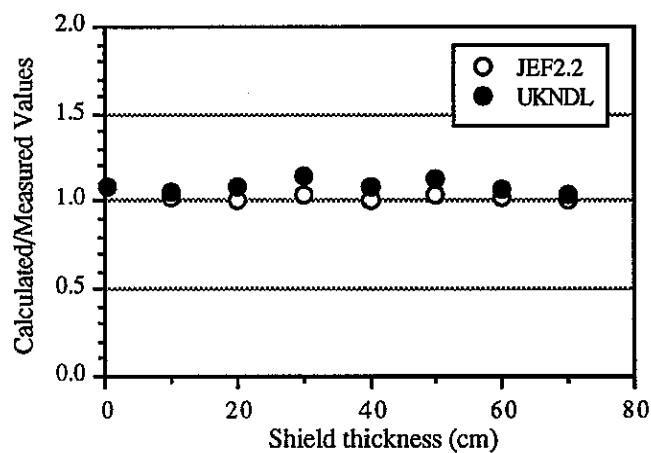


Figure 10 Graphite Benchmark C/M Values for S32 Detector

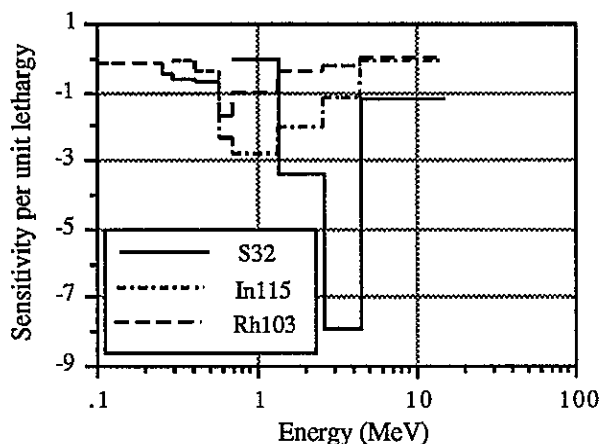


Figure 9 Iron Benchmark Sensitivities to Total iron cross-section after 46cm of Mild Steel

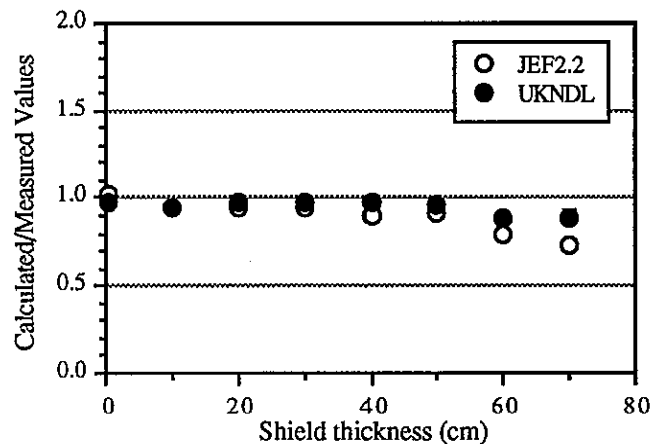


Figure 11 Graphite Benchmark C/M Values for In115 Detector

B. Graphite Benchmark

Figures 10-12 show C/M values obtained for the three threshold detectors used in the graphite benchmark for both JEF2.2 and UKNDL data. The JEF2.2 data consistently give lower reaction rates than the UKNDL data: in the case of the S32(n,p)P32 detector this represents improved agreement with experiment but for the In115(n,n')In115m and Rh103(n,n')Rh103m detectors the results are worse than with UKNDL data. The results for the In115(n,n')In115m and Rh103(n,n')Rh103m detectors show an overprediction of attenuation through the shield whilst those for the S32(n,p)P32 detector agree well with experiment. Figure 13 shows the sensitivities of the three detector reaction rates after 70cm to the total carbon cross-section. Combining the sensitivities with the detector results suggests qualitatively that there may be problems with the JEF2.2 carbon cross-sections in the energy range

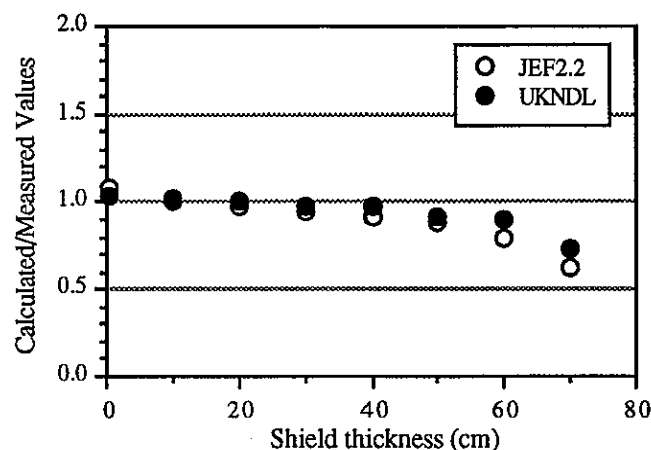


Figure 12 Graphite Benchmark C/M Values for Rh103 Detector

0.8MeV to 2.9MeV, where the indium and rhodium sensitivities are high compared with those for sulphur.

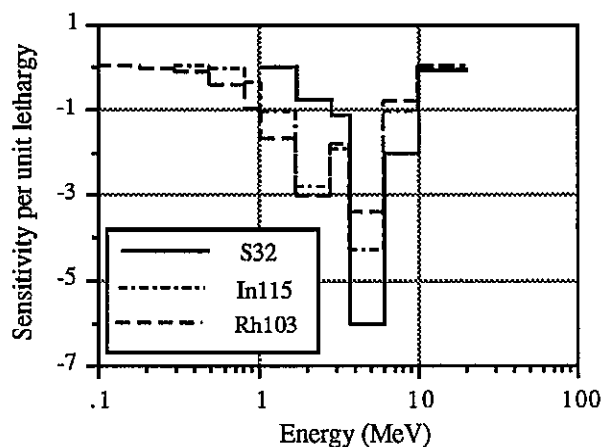


Figure 13 Graphite Benchmark Sensitivities to Total carbon cross-section after 70cm of Graphite

C. Water Benchmark

Figure 14 shows the C/M values obtained for the S32(n,p)P32 detector in the water benchmark using JEF2.2 data : no UKNDL results were available for comparison. The error bars in Figure 14 include uncertainty due to reproducibility of the measurements. The reaction rate is overpredicted but the attenuation is well predicted, indicating that the discrepancy is not caused by cross-section deficiencies. Figures 15-16 show C/M values for the spectra above 1MeV obtained at penetrations of 10.2cm and 50.8cm. The standard deviations are quite large but there is no indication of cross-section deficiency between 1.7MeV and 8.8MeV, the same being true for other penetrations. There may be a problem with the data above 8.8MeV. Thus the JEF2.2 hydrogen and oxygen cross-sections in the range 1.7MeV to 8.8MeV appear to be good.

D. NESDIP2 Benchmark

Figures 17-19 show the C/M values obtained for the three threshold detectors in the NESDIP2 benchmark, together with the corresponding results obtained with UKNDL data. The JEF2.2 results in the mild steel simulating the pressure vessel and in the cavity are higher than those obtained using UKNDL data; this is consistent with the observations in the iron benchmark and represents improved agreement with experiment. The JEF2.2 results are reasonably good, the reaction rates generally being underpredicted with a maximum underprediction of 16% for the In115(n,n')In115m and Rh103(n,n')Rh103m detectors in the cavity. This underprediction may be a reflection of the possible problems with iron data mentioned previously. Generally, however, the JEF2.2 data appears to be acceptable for this simulation of a practical shield.

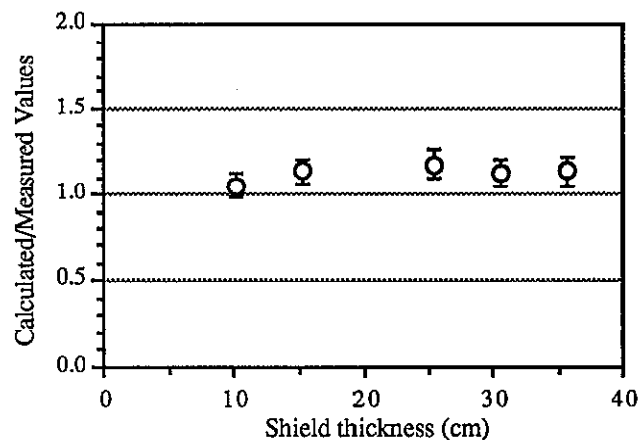


Figure 14 Water Benchmark C/M Values for S32 Detector

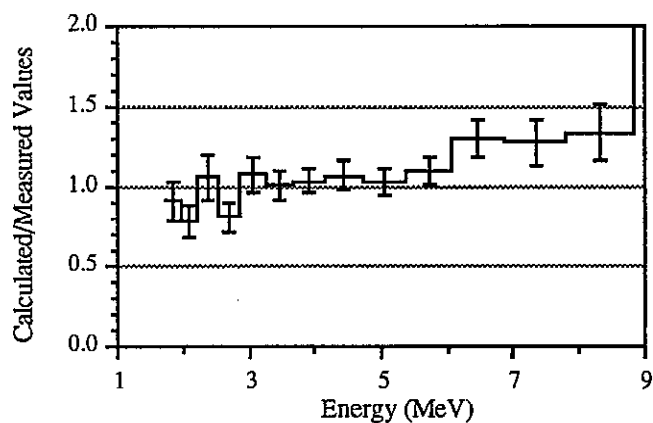


Figure 15 Water Benchmark C/M Values for Neutron Flux after 10cm penetration

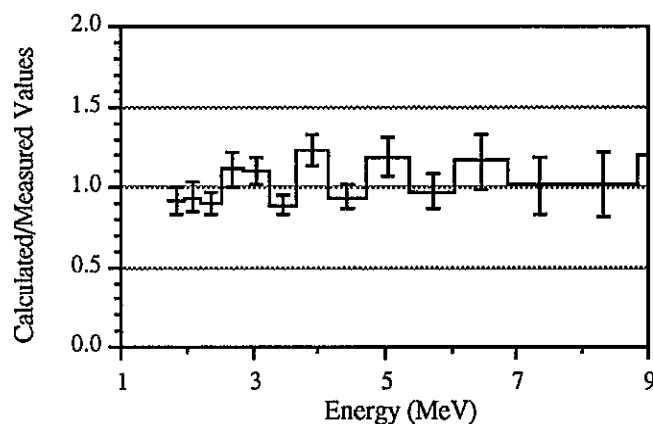


Figure 16 Water Benchmark C/M Values for Neutron Flux after 51cm penetration

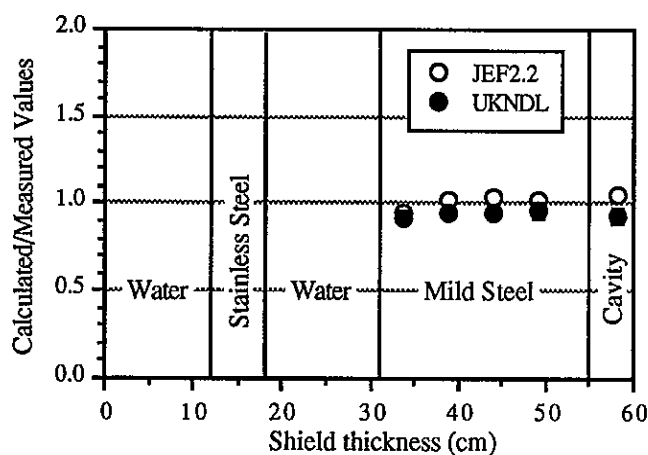


Figure 17 NESDIP2 Benchmark C/M Values for S32 Detector

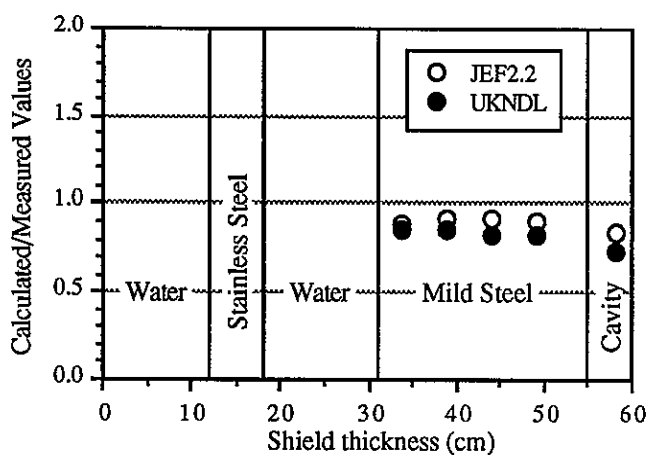


Figure 18 NESDIP2 Benchmark C/M Values for In115 Detector

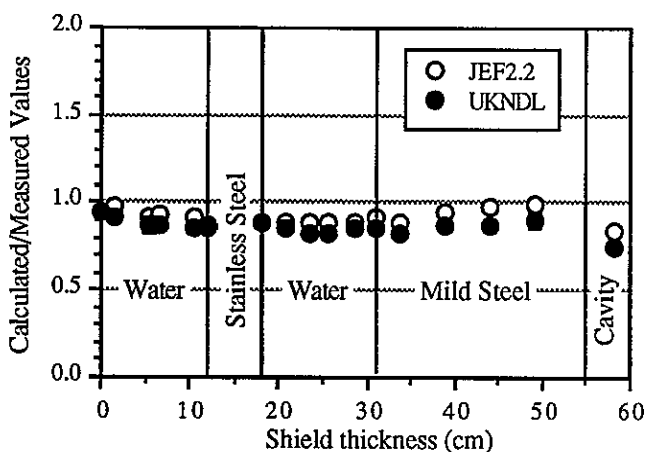


Figure 19 NESDIP2 Benchmark C/M Values for Rh103 Detector

Table 1
Iron Benchmark. Ratio of results using shielded Fe56 cross-sections to those using infinitely dilute cross-sections

Shield thickness	S32	sd	In115	sd	Rh103	sd
0.0 cm	0.98	0.02	0.99	0.02	0.99	0.01
10.2 cm	1.00	0.02	1.02	0.02	1.04	0.01
20.4 cm	1.00	0.02	1.10	0.03	1.13	0.02
30.8 cm	1.04	0.03	1.22	0.04	1.25	0.02
41.2 cm	1.07	0.03	1.42	0.06	1.31	0.02
51.6 cm	1.14	0.04	1.70	0.07	1.40	0.05
56.7 cm	1.19	0.04	1.77	0.07	1.51	0.03
67.0 cm	1.08	0.05	2.16	0.14	1.65	0.05

Table 2
NESDIP2 Benchmark. Ratio of results using shielded Fe56 cross-sections to those using infinitely dilute cross-sections

Shield thickness	S32	sd	In115	sd	Rh103	sd
0.0 cm	1.01	0.01	0.99	0.02	0.98	0.02
6.6 cm	0.99	0.02	1.01	0.02	1.06	0.03
12.1 cm	0.99	0.02	1.00	0.03	1.00	0.03
18.0 cm	1.00	0.02	1.00	0.02	1.00	0.02
25.7 cm	1.03	0.02	1.03	0.02	1.03	0.02
31.2 cm	0.99	0.02	1.00	0.02	1.00	0.02
38.8 cm	1.01	0.02	1.02	0.02	1.02	0.02
43.9 cm	1.03	0.03	1.06	0.02	1.05	0.02
49.0 cm	1.04	0.03	1.08	0.02	1.07	0.02
58.1 cm	1.03	0.04	1.12	0.02	1.15	0.02

E. Resonance Shielding Effects in Fe56

Tables 1 and 2 show the ratio of results obtained in the iron and NESDIP2 benchmarks using the recommended totally shielded Fe56 cross-sections to those obtained using infinitely dilute Fe56 cross-sections. The differences between results indicate the extent of the within-group resonance shielding effect for these configurations with the 1/128 lethargy energy group scheme used in the Fe56 resonance region in MCBEND. As one would expect, the effect for the intermediate energy detectors, In115(n,n')In115m and Rh103(n,n')Rh103m is higher than that for the high energy S32(n,p)P32 detector since they are more sensitive to the Fe56 resonance region. For the iron benchmark the effect on the indium and rhodium reaction rates is severe, with ratios at the back of the shield of 2.16 and 1.65, respectively. The effect in the NESDIP2 experiment, with a smaller amount of Fe56 present, is, of course, much lower. At the front face of the simulated pressure vessel it has no effect at all but the change increases to maximum ratios in the cavity of 1.12 and 1.15

for the indium and rhodium detectors. These results confirm that the 1/128 lethargy energy group scheme is not fine enough to be regarded as point energy in the Fe56 resonance region with the resonance shielding effect being up to 15% in a simulated PWR radial shield. A useful extension to this work would be to gradually refine the group scheme to ascertain what lethargy width is required for the group scheme to be equivalent to point energy.

V. CONCLUSIONS

The new JEF2.2 nuclear data library is currently being benchmarked for shielding applications by analysing Winfrith benchmark experiments using the Monte Carlo code MCBEND. Three single material benchmarks, in iron, graphite and water and a multi-material benchmark consisting of an iron/water shield have been analysed so far, with the following main conclusions.

The JEF2.2 iron data give good results for $S32(n,p)P32$, $Rh103(n,n')Rh103m$ and $Au197(n,\gamma)Au198$ /Cd reaction rates through up to 67cm of mild steel but poorer results for $In115(n,n')In115m$ reaction rates suggest possible errors in the cross-sections of iron between 0.6MeV and 1.4MeV.

The JEF2.2 iron data give improved results compared with UKNDL data in mild steel.

The JEF2.2 carbon data give good results for $S32(n,p)P32$ reaction rates but overpredict the attenuation of $In115(n,n')In115m$ and $Rh103(n,n')Rh103m$ reaction rates through 70cm of graphite, indicating a possible problem with the data between 0.8MeV and 2.9MeV.

JEF2.2 carbon data give lower results than UKNDL data : at high energies this represents an improvement but at intermediate energies the agreement with measurement is worse.

JEF2.2 hydrogen and oxygen data appear to be adequate between 1.7MeV and 8.8MeV for calculating penetration through up to 50cm of water.

For an iron/water benchmark simulating the radial shield of a PWR the JEF2.2 data is adequate, with values of C/M of 1.04, 0.92 and 0.97, respectively, for $S32(n,p)P32$, $In115(n,n')In115m$ and $Rh103(n,n')Rh103m$ reaction rates in the middle of the vessel. Agreement becomes worse in the cavity with underprediction by 16% of the $In115(n,n')In115m$ and $Rh103(n,n')Rh103m$ reaction rates.

JEF2.2 data give results which are higher than those using UKNDL data in the pressure vessel and cavity of the iron/water benchmark. This trend represents improved agreement with experiment and is consistent with that observed in the iron benchmark.

The energy group scheme used by MCBEND above 72eV (1/128 lethargy width), is not fine enough to eliminate all dependence on resonance shielding in Fe56, particularly in the problematic unresolved region. Totally shielded cross-sections are the best approximation to the correct weighting in this scheme and are recommended. The effect of resonance shielding with this group scheme is most marked in the iron benchmark. In the simulation of the PWR radial shield the effect is negligible at the front of the vessel but rises to 15% in the cavity for the $Rh103(n,n')Rh103m$ reaction rate. Calculations with a finer group scheme would be useful to determine the lethargy width required to make the data equivalent to point energy.

ACKNOWLEDGEMENTS

The work described in this paper was funded under the UK Health and Safety Executive Nuclear Safety Research programme.

REFERENCES

1. S.J.Chucas, I.J.Curl and P.C.Miller, "The advanced features of the Monte Carlo code MCBEND", *Seminar on Advanced Monte Carlo Computer Programs for Radiation Transport*, OECD/NEA, Paris, 1993
2. M.C.G.Hall, "DUCKPOND - a perturbation Monte Carlo code and its applications", *Proc. OECD Specialists' Meeting on Nuclear Data and Benchmarks for Reactor Shielding*, OECD, Paris 1980
3. R.E.Macfarlane, "Introducing NJOY89", *Proc. Seminar on NJOY and THEMIS*, p 7-35, OECD/NEA, Paris, 1989
4. D.E.Cullen and P.K.McLaughlin, "The International Reactor Dosimetry File (IRDF85)", IAEA-ND5-41
5. P.C.Miller, G.A.Wright, C.B.Boyle and S.W.Power, "The use of an inbuilt importance generator for acceleration of the Monte Carlo code MCBEND", *Proc. International Conference on the Physics of Reactors : Operation Design and Computation, Volume 3*, p II-124 - II-132, American Nuclear Society, Marseille, 1990